VI International Conference on Computational Methods for Coupled Problems in Science and Engineering
COUPLED PROBLEMS 2015
B. Schrefler, E. Oñate and M. Papadrakakis(Eds)

A SENSITIVITY BASED OPTIMIZATION APPROACH FOR AEROACOUSTIC PROBLEMS

STEFANIE NOWAK*, DÖRTE C. STERNEL* AND MICHAEL SCHÄFER*

*Institute of numerical Methods in Mechanical Engineering, TU Darmstadt,
Dolivostrasse 15, 64293 Darmstadt, Germany
e-mail: nowak@fnb.tu-darmstadt.de, web page: http://www.fnb.tu-darmstadt.de/

Key words: aeroacoustics, gradient-based optimization, sensitivity equations, finite-volume method

Abstract. This paper proposes an approach for the sensitivity computation of an aeroacoustic problem via the solution of the continuous sensitivity equations. The equations are derived by differentiating the coupled system (Navier-Stokes equations and the linearized Euler equations) with respect to design parameters. The obtained acoustic sensitivity information can be used to analyze the flow control variable's influence on the acoustic field or to calculate the gradient of an objective functional within aeroacoustic optimization problems. The components of the coupled sensitivity solver are systematically verified.

1 INTRODUCTION

The prediction and optimization of noise generated by fluid flow is of high interest in numereous fields in industry and current research. Many occurances in the aeroacoustics field are related to low-speed flows, e.g. wind turbines or automobile's noise. Numerical simulations of aeroacoustic problems support practical experiments and provide eligible measurements for noise reduction.

The sound prediction can be based on the simulation of the compressible Navier-Stokes equations (direct noise computation, DNC). DNC is inefficient for low Mach number flows, because of the different spatial and temporal scales in the fluid flow and the acoustics. Hybrid approaches consider the flow and the acoustic field separately and, therefore, are cost saving. Lighthill's acoustic analogy [1] and his further work [2] were important milestones in the aeroacoustics discipline. Alternatively to the acoustic analogies splitting approaches are considered. In [3] the acoustic/viscous splitting is introduced. Here, the compressible field is considered as the superposition of an incompressible flow with an acoustic perturbation. The flow is computed via the incompressible Navier-Stokes equations. Shen and Sørensen proposed a modified version of the method in [4], where the sound field is obtained with the linearized Euler equations.

However, not only the behavior of the flow and the originated sound is of interest, but how to affect the flow and consequently the sound to reach given aims. An objective could be, for instance, to minimize the sound intensity in a given area.
Optimization methods for the resolution of minimization problems can be divided into strategies without and with determination of the cost functional's derivative. An efficient possibility of computing this gradient is to solve the continuous sensitivity equations (CSE). These equations arise from differentiating the state equations with respect to a design parameter. In [5] an outline of sensitivity analysis of flow problems is presented and Gunzburger [6] discusses sensitivity analysis in the context of flow control and optimization. In addition to the CSE method, there is the discrete sensitivity equation approach, in which the total derivative of the flow approximation with respect to the design parameter is calculated. In Kleiber et al. [7] a discussion of the two approaches is found.
A method for computing transient flow sensitivities with the CSE method is presented by Ilinca et al. [8] and Hristova et al. [9]. After extensive research the authors have not found any application of the continuous sensitivity equation method for the LEE in any scientific contents.
This paper presents the theoretical background of the CSE of a coupled aeroacoustics problem. The coupling of the sensitivity equations and verification test cases of each component of the coupled solver are considered.

2 GOVERNING EQUATIONS

The aeroacoustic equations are derived via employment of the expansion about incompressible flow proposed by Shen and Sørensen [4] and are further developed by Kornhaas [10]. Here the compressible flow field at low Mach numbers is composed of an incompressible backround flow (superscript *inc*) with a superimposed acoustic perturbation (superscript *ac*). The Einstein summation convention is used throughout the paper. The composition is given by

$$\rho = \rho^{inc} + \rho^{ac}, \qquad u_i = u_i^{inc} + u_i^{ac}, \qquad p = p^{inc} + p^{ac}, \tag{1}$$

with density ρ, velocity u_i and pressure p. The following paragraphs describe the models for the incompressible flow and the acoustics.

Flow equations The incompressible and unsteady fluid flows are modelled by the Navier-Stokes equations (NSE) [11]. The conservation equations of mass and momentum can be written as

$$\frac{\partial u_i^{inc}}{\partial x_i} = 0, \tag{2}$$

$$\rho^{inc}\frac{\partial u_i^{inc}}{\partial t} + \rho^{inc}\frac{\partial u_i^{inc} u_j^{inc}}{\partial x_j} = \frac{\partial \tau_{ij}^{inc}}{\partial x_j} - \frac{\partial p^{inc}}{\partial x_i} + \rho^{inc} f_i, \tag{3}$$

with the time t, Cartesian coordinates x_i and the external body forces f_i. With the dynamic viscocity μ the stress tensor is given by

$$\tau_{ij}^{inc} = \mu \left(\frac{\partial u_i^{inc}}{\partial x_j} + \frac{\partial u_j^{inc}}{\partial x_i} \right). \tag{4}$$

Acoustic equations Under the assumption that the acoustic variables are small compared to the flow variables, the linearized Euler equations (LEE) [12] are used to obtain the acoustic variables.

The LEE are given by

$$\frac{\partial \rho^{ac}}{\partial t} + \rho^{inc} \frac{\partial u_i^{ac}}{\partial x_i} + u_i^{inc} \frac{\partial \rho^{ac}}{\partial x_i} = 0, \tag{5}$$

$$\rho^{inc} \frac{\partial u_i^{ac}}{\partial t} + \rho^{inc} u_j^{inc} \frac{\partial u_i^{ac}}{\partial x_j} + \frac{\partial p^{ac}}{\partial x_i} = 0, \tag{6}$$

$$\frac{\partial p^{ac}}{\partial t} + c^2 \rho^{inc} \frac{\partial u_i^{ac}}{\partial x_i} + c^2 u_i^{inc} \frac{\partial \rho^{ac}}{\partial x_i} = \frac{\partial p^{inc}}{\partial t}, \tag{7}$$

with the speed of sound c.

3 GRADIENT BASED OPTIMIZATION

A general aeroacoustic optimization problem is composed of a given objective functional $\mathcal{J}$ depending on flow state variables ϕ, for example, fluid velocity or pressure and acoustic state variables ψ, for example, the sound pressure or the particle velocity. Both state variables depend on the design variables $\mathbf{a}$, for example, the inlet velocity of the flow or shape parameters. Mathematically an aeroacoustic optimization problem can be formulated as

$$\min_{\mathbf{a} \in \mathbb{R}^\mathbf{n}} \mathcal{J}(\psi(\mathbf{a}), \mathbf{a}) \quad \text{subject to} \quad \begin{cases} \mathbf{F}(\phi(\mathbf{a}), \mathbf{a}) = \mathbf{0} \\ \mathbf{A}(\psi(\mathbf{a}), \phi(\mathbf{a}), \mathbf{a}) = \mathbf{0}. \end{cases} \tag{8}$$

Here, the constraints $\mathbf{F} = \mathbf{0}$ and $\mathbf{A} = \mathbf{0}$ are the governing equations of the fluid and the acoustics. Other side constraints are possible, like restrictions to the inlet velocity. The objective function $\mathcal{J}$ is an essential concept in optimization problems. It describes what is to be optimized, for instance, the sound intensity. $\mathcal{J}$ is usually not directly dependent on the design variables, but via the acoustic state variables $\mathcal{J}$ depends indirectly on the design variables.

Calculation of the objective function's gradient Gradient-based optimization methods use information about the objective function's gradient and its evaluations. The *i-th* component of the gradient of the objective function can be written as

$$\frac{d\mathcal{J}}{da_i} = \frac{\partial \mathcal{J}}{\partial \psi_i} \frac{\partial \psi_j}{\partial a_i} + \frac{\partial \mathcal{J}}{\partial a_i}. \tag{9}$$

$d\mathcal{J}/da_i$ denotes the total derivative of the objective function with respect to the design parameter a_i. In this case, the objective function depends only on the acoustic variables and the control variables. In Eq. (9) the term $\partial\psi_j/\partial a_i$, the sensitivity with respect to a design parameter a_i, is rather complicated to compute. There are several procedures for computing the sensitivities of flow and acoustics. The next section shows one of these methods for the continuous sensitivities, starting with the theoretical background of the coupling, and thereafter, the derivation of the continuous aeroacoustic sensitivity equations.

4 COUPLED SENSITIVITY EQUATION SYSTEM

To obtain the CSE system the constraints in (8) have to be differentiated with respect to the design parameters. This leads to the following equations

$$\frac{\partial \mathbf{F}}{\partial \mathbf{a}} + \frac{\partial \mathbf{F}}{\partial \phi}\frac{d\phi}{d\mathbf{a}} = 0, \tag{10}$$

$$\frac{\partial \mathbf{A}}{\partial \mathbf{a}} + \frac{\partial \mathbf{A}}{\partial \phi}\frac{d\phi}{d\mathbf{a}} + \frac{\partial \mathbf{A}}{\partial \psi}\frac{d\psi}{d\mathbf{a}} = 0. \tag{11}$$

For the purposes of simplicity, the following abbreviation is introduced

$$\phi_k = \frac{\partial \phi}{\partial a_k}. \tag{12}$$

Differentiation of the unsteady Navier-Stokes equations (2)-(3) with respect to the k-th design parameter a_k results in the unsteady continuous sensitivity equations of the unsteady NSE. In consideration of the chain rule, permutation of the differential operators and notation (12) the equations are given by

$$\frac{\partial u_{j,k}^{inc}}{\partial x_j} = 0, \tag{13}$$

$$\rho\frac{\partial u_{i,k}^{inc}}{\partial t} + \frac{\partial}{\partial x_j}\left(\rho u_{i,k}^{inc}u_j^{inc} + \rho u_i^{inc}u_{j,k}^{inc}\right) - \frac{\partial}{\partial x_j}\left[\mu\left(\frac{\partial u_{i,k}^{inc}}{\partial x_j} + \frac{\partial u_{j,k}^{inc}}{\partial x_i}\right)\right] = \frac{\partial p_k^{inc}}{\partial x_i}, \tag{14}$$

assuming, that the material properties ρ and μ are constant and the volume force is insensitive to external influences. The boundary conditions for the CSE are obtained by differentiation of the corresponding boundary conditions for the NSE with respect to the design parameter a.

The sensitivity equations of the linearized Euler equations are obtained via differentiation of the linearized Euler equations with respect to the *k-th* design variable a_k. Hence differentiation of (5)-(7) yields to

$$\begin{aligned}
\frac{\partial \rho_k^{ac}}{\partial t} + \rho^{inc}\frac{\partial u_{i,k}^{ac}}{\partial x_i} + u_i^{inc}\frac{\partial \rho_k^{ac}}{\partial x_i} &= -u_{i,k}^{inc}\frac{\partial \rho^{ac}}{\partial x_i}, && (15)\\
\rho^{inc}\frac{\partial u_{i,k}^{ac}}{\partial t} + \rho^{inc}u_j^{inc}\frac{\partial u_{i,k}^{ac}}{\partial x_j} + \frac{\partial p_k^{ac}}{\partial x_i} &= -\rho^{inc}u_{j,k}^{inc}\frac{\partial u_i^{ac}}{\partial x_j}, && (16)\\
\frac{\partial p_k^{ac}}{\partial t} + c^2\rho^{inc}\frac{\partial u_{i,k}^{ac}}{\partial x_i} + c^2 u_i^{inc}\frac{\partial \rho_k^{ac}}{\partial x_i} &= \frac{\partial p_k^{inc}}{\partial t} - c^2 u_{i,k}^{inc}\frac{\partial \rho^{ac}}{\partial x_i}. && (17)
\end{aligned}$$

The obtained equations have the same form as the LEE. Additional terms can be considered as additional source terms. The coupling between sensitivity equations for flows and acoustics is realized by these terms using flow sensitivities and acoustic variables.

5 NUMERICAL METHODS

The numerical solution of the coupled system is realized as an integrated procedure, see Figure 1. The acoustic sensitivities do not influence the flow sensitivities.

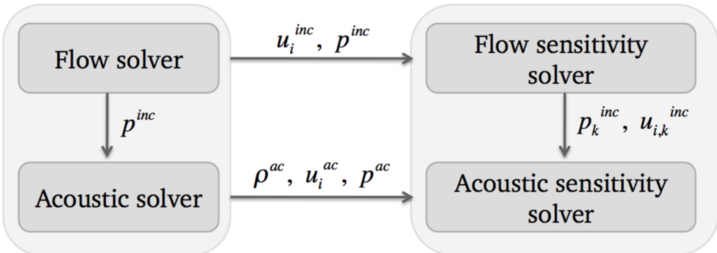

Figure 1: Numerical realization of the coupled approach as an integrated procedure

Before computing the flow sensitivities and the acoustic sensitivities, the NSE (2)-(3) and LEE (5)-(7) have to be solved. This is done by using our in-house solver FASTEST which applies a fully conservative finite-volume approach to solve the incompressible NSE and the linearized Euler-equations on a collocated, block structured and cell centered grid [12, 13]. After each time-step the flow and acoustic quantities are transferred to the sensitivity solver via MPI (Message Passing Interface).

Flow sensitivity solver Analogously to the Navier-Stokes equations the spatial discretization of the sensitivity equations utilizes the finite-volume method. The discretization of the sensitivity equations of the NSE for steady problems can be read in detail in [15] and [16]. The unsteady sensitivity equations contain one additional term:

$$\rho\frac{\partial u_{i,k}^{inc}}{\partial t}. \qquad (18)$$

The time discretization is performed with an implicit Euler scheme of first and second order.

Acoustic sensitivity solver Analogously to the linearized Euler equations the acoustic sensitivities are computed via a high-resolution scheme, which solves a Riemann problem at the cell faces. The high-resolution scheme combines the second-order Lax-Wendroff method and the first order Godunov method with the help of flux-limiters. Kornhaas presents the high-resolution scheme in detail [10]. The time discretization is done with first and second order implicit Euler scheme.

6 VERIFICATION

To verify the implemented method, the numerical order achieved is compared to the analytical order for each method of the coupled code. At first, the order of the unsteady continuous sensitivity equation's discretization method is presented followed by the order of the sensitivity equations of the linearized Euler equations method.
To assess the solution quality, the error

$$e_h = p^{ac}_{num,h} - p^{ac}_{ana} \tag{19}$$

is considered, where p^{ac}_{num} is the numerically computed sound pressure and p^{ac}_{ana} is the analytical sound pressure. The discrete L_2-norm of the error is defined by

$$\|e\|_{h,L_2} = \sqrt{\frac{1}{N}\sum_{i=1}^{N} e_h^2}, \tag{20}$$

where N is the number of control volumes.

6.1 Verification of the acoustic sensitivity equations

The first verification test case is calculated without background flow ($u_i^{inc} = 0$). The computational domain and the initial location of the sound wave are presented in Figure 2. The computations are done on four grid levels with 16384, 8192, 4096 and 2046 control volumes in x-direction.
The initial values of the acoustic quantities are as follows:

$$p^{ac} = 2^{-1200(x-0.25)^2}, \tag{21}$$

$$u^{ac} = 0.001 \cdot 2^{-1200(x-0.25)^2}, \tag{22}$$

$$v^{ac} = 0, \tag{23}$$

$$\rho^{ac} = 0. \tag{24}$$

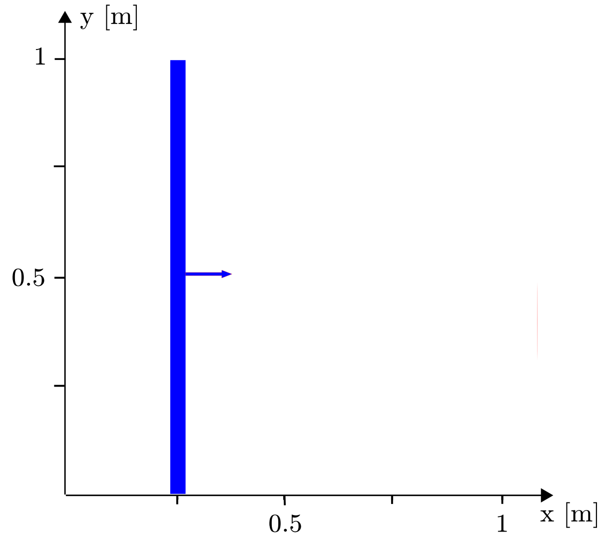

Figure 2: Domain and initial location of the sound wave.

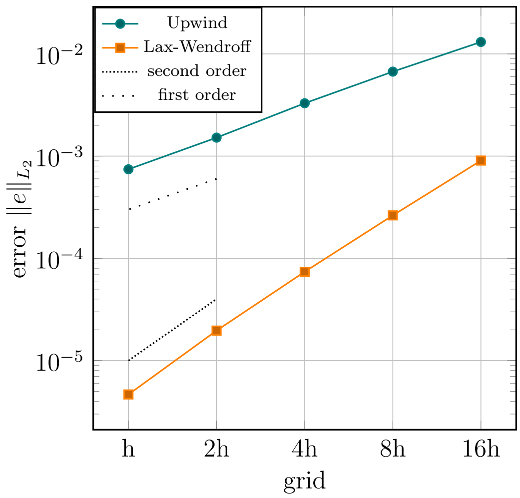

Figure 3: L_2-error depending on the grid for different methods

The wave starts at $x = 0.25$ m. The density is $\rho^{inc} = 1000$ kg/m^3 and the dynamic viscosity is $\mu^{inc} = 10^{-5}$ kg/m s. The corresponding speed of sound is $c = 1$ m/s. The resulting orders are illustrated in Figure 3. One can see that the upwind-scheme converges to an order of one, whereas the Lax-Wendroff scheme converges to an order of two.

6.2 Verification of the flow sensitivity equations

In this section the time discretization scheme implemented in the flow sensitivity solver is verified using the method of manufactured solutions (MMS) [17]. The order of the spatial discretization for the steady NSE is presented in [15]. Direct differentiation of the manufactured solution for the flow provides closed-form expressions for the sensitivities. A time convergence study is performed to assess the temporal accuracy of the sensitivity solutions.

We choose the following exact solution of the unsteady NSE, which is also the inflow boundary condition and depends on the design parameter a:

$$u_{in}(x,y) = a\cos(5t)\sin\left(\frac{\pi x}{2}\right)\cos\left(\frac{\pi y}{2}\right), \tag{25}$$

$$v_{in}(x,y) = -a\cos(5t)\cos\left(\frac{\pi x}{2}\right)\sin\left(\frac{\pi y}{2}\right). \tag{26}$$

$$\tag{27}$$

Differentiation with respect to the design parameter a gives the sensitivities

$$u_k(x,y) = \cos(5t)\sin\left(\frac{\pi x}{2}\right)\cos\left(\frac{\pi y}{2}\right), \tag{28}$$

$$v_k(x,y) = -\cos(5t)\cos\left(\frac{\pi x}{2}\right)\sin\left(\frac{\pi y}{2}\right). \tag{29}$$

$$\tag{30}$$

The computational domain and the sensitivities are shown in Figure 4 and Figure 5.

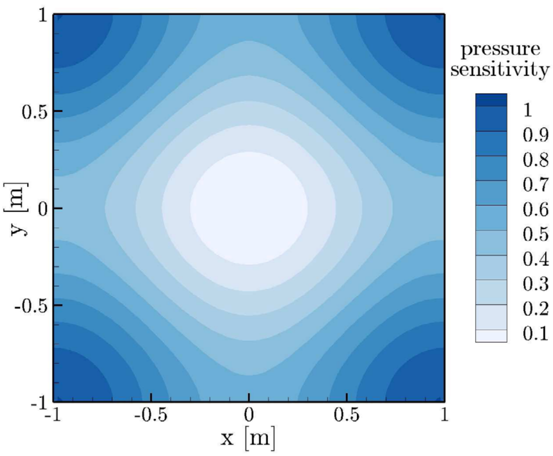

Figure 4: Domain and pressure sensitivity for $t = 0$ s.

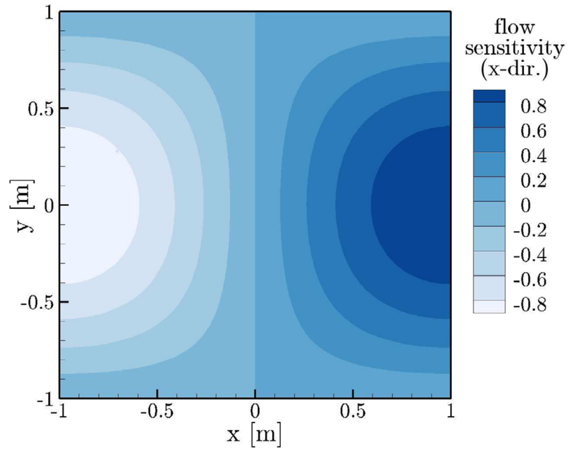

Figure 5: Domain and flow sensitivity in x-direction for $t = 0$ s.

Table 1 shows the time step sizes and the results for the order of the flow sensitivities for the first order implicit Euler scheme. The order of the pressure computation is illustrated at the left side, whereas on the right sight the order of the velocity computation is shown. The order of the pressure and the order of the velocity converge to one. In Table 2 the orders of the pressure and the velocity for the second order implicit Euler scheme are presented. Both orders converge to two.

Table 1: Order of accuracy of the flow sensitivities for the first order implicit Euler scheme

time step size	pressure	order
0.005	0.46531836731	
0.0025	0.47096579783	
0.00125	0.47380853834	0.9903
0.000625	0.47523497813	0.995
0.0003125	0.47594950138	0.998

time step size	u velocity	order
0.005	-0.78628698376	
0.0025	-0.78631729909	
0.00125	-0.78633378171	0.89
0.000625	-0.78634240443	0.93
0.0003125	-0.78634681860	0.97

Table 2: Order of accuracy of the flow sensitivities for the second order implicit Euler scheme

time step size	pressure	order
0.005	0.47917358818	
0.0025	0.47838279892	
0.00125	0.47846168824	2.43
0.000625	0.47847809934	2.27
0.0003125	0.47848192570	2.10

time step size	u velocity	order
0.005	-0.78633065815	
0.0025	-0.78636059225	
0.00125	-0.78636832215	1.95
0.000625	-0.78637006368	2.15
0.0003125	-0.78637047477	2.08

6.3 Comparison of the acoustic sensitivities with the corresponding difference quotient

The acoustic sensitivity solver can be verified by estimating the gradients of the acoustic quantities with respect to a using finite differences (FD). When computing FD the design parameter a is changed by a small amount δa and the solution is recomputed. In this test case only the sensitivity of the acoustic pressure and its difference quotient with respect to a are considered. As a first step, the flow sensitivities are left out. A pressure pulse and its sensitivities are prescribed as input for the sensitivity equations of the LEE:

$$p^{inc} = 10^3 e^{-10^2(x^2+y^2)} cos(200\pi t)\ a, \tag{31}$$

$$p_k^{inc} = 10^3 e^{-10^2(x^2+y^2)} cos(200\pi t). \tag{32}$$

The reference FD acoustic sensitivities are estimated by

$$\left(\frac{\partial p^{ac}}{\partial a}\right)_{FD} = \frac{p^{ac}(a+\delta a) - p^{ac}(a-\delta a)}{2\delta a} + \mathcal{O}(\delta a^2). \tag{33}$$

In the following comparison $\delta a = 10^{-3}$ is chosen. The computational domain is illustrated in Figure 6. As boundary conditions an acoustic outlet is used on each boundary. The grid consists of 128 control volumes in x- and y-direction. The Courant number for the acoustic computation is 0.1. The acoustic pressure sensitivity and the acoustic pressure are monitored at point P$(0, 0.5)$. The difference quotient and the sensitivity of the acoustic pressure in P are shown in Figure 7. The comparison shows a good agreement between the sensitivity and the difference quotient. Only minor differences of the gradients are perceptible.

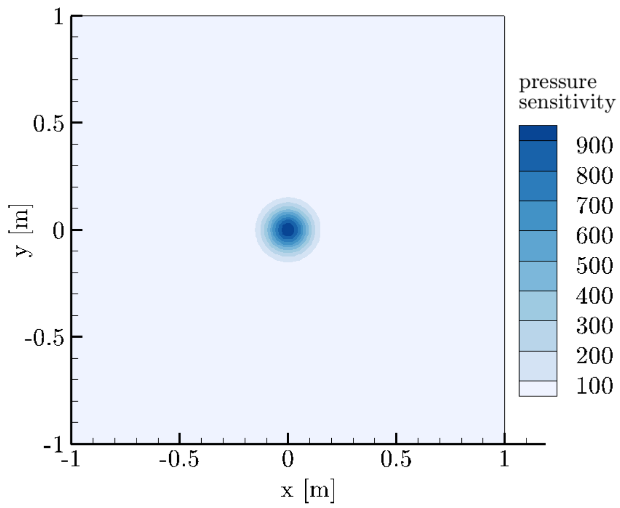

Figure 6: Domain and pressure sensitivity for $t = 0$ s.

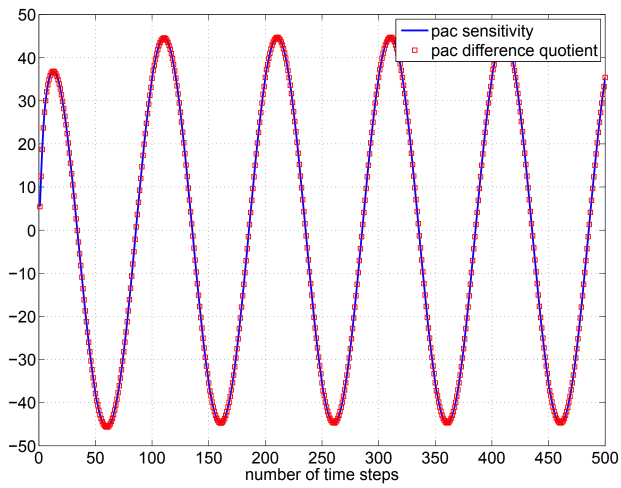

Figure 7: Difference quotient and the sensitivity of the acoustic pressure in P after $t = 0.05$ s.

7 CONCLUSION

A general sensitivity based optimization approach for aeroacoustic problems has been presented. We introduced the basic equations describing flow and acoustics, a general optimization problem, and the gradient computation with a coupled sensitivity solver. Furthermore, we presented the mathematical background for the derivation of the unsteady sensitivity equations from the Navier-Stokes equations, and the linearized Euler equations. Hereafter, the mathematical coupling of the solver was shown. In a first step the numerical results of the sensitivity computation could be verified for each component of the coupled solver via investigation of the order and the comparison with a finite difference approach. The obtained sensitivity values enable a deeper understanding of the whole system and provide information about the influence of all flow parameters on the acoustics. For further investigations, a test case of acoustic sensitivities based on flow sensitivity computation will be considered and an optimization test case with sensitivities will be computed.

REFERENCES

[1] Lighthill, M. *On Sound Generated Aerodynamically. I. General Theory.* Proceedings of The Royal Societey London A, 1952

[2] Lighthill, M. *On Sound Generated Aerodynamically. II. Turbulence as a source of sound.* Proceedings of The Royal Societey London A, 1954

[3] Hardin, J.C. and Pope, D.S. *An Acoustic/Viscous Splitting Technique for Computational Aeroacoustics.* Theoretical and Computational Fluid Dynamics 6, 1994

[4] Shen, W. and Soerensen, J. *Comment on the aeroacoustic formulation of Hardin and Pope.* AIAA Journal, 1999

[5] Stanley, L.G. and Stewart, D.L. *Design sensitivity analysis.* Society for Industrial and Applied Mathematics, Philadelphia, 2002

[6] Gunzburger, M.D. *Perspectives in flow control and optimization.* Society for Industrial and Applied Mathematics, Philadelphia, 2003

[7] Kleiber, M. and Antunez, H. and Hien, T.D. *Parametric Sensitivity in Nonlinear Mechanics.* Whiley, New York, 1997

[8] Ilinca, F. and Hay, A. and Pelletier, D. *Shape sensitivity analysis of unsteady laminar flow past a cylinder in ground proximity.* AIAA Fluid Dynamics Conference and Exhibit, 2006.

[9] Hristova, H. and Etienne, S. and Pelletier, D. and Borggaard, J. *A continuous sensitivity equation method for time-dependent incompressible laminar flows.* International Journal for Numerical Methods in Fluids, 2006

[10] Kornhaas, M. *Effiziente numerische Methoden fr die Simulation aeroakustischer Probleme mit kleinen Machzahlen.* Ph.D. dissertation, TU Darmstadt, 2012

[11] Schäfer, M. *Computational Engineering - Introduction to Numerical Methods.* Springer, 2006

[12] Kornhaas, M. and Sternel, D.C. and Schäfer, M. *Efficient numerical simulation of aeroacoustics for low Mach number flows interacting with structures.* Computational Mechanics, to appear

[13] Durst, F. and Schäfer, M. *A parallel block-structured multigrid method for the prediction of incompressible flows.* 1996

[14] Leveque, R.J. *Finite Volume Methods for Hyperbolic Problems.* Cambridge Texts in Applied Mathematics, 2002

[15] Michaelis, J. *Parallele Mehrgitter-Strategien zur Sensitivitätsanalyse und Strömungsoptimierung.* Ph.D. dissertation, TU Darmstadt, 2012

[16] Siegmann, J. *Sensitivitätsanalyse zur gradientenbasierten Formoptimierung von Strömungsproblemen.* Ph.D. dissertation, TU Darmstadt, 2012

[17] Salari, K. and Knupp, P. *Code Verification by the Method of Manufactured Solutions.* Technical Report SAND2000 - 1444, Sandia National Laboratories, 2000 International Journal for Numerical Methods in Fluids, 1996